

High-pressure phase transitions in CaTe and SrTe

H. G. Zimmer, H. Winzen, and K. Syassen

Physikalisches Institut III, Universität Düsseldorf, D-4000 Düsseldorf 1, Federal Republic of Germany

(Received 14 November 1984; revised manuscript received 25 March 1985)

Pressure-volume relationships and structural transitions in CaTe and SrTe are investigated at high pressure using x-ray diffraction. SrTe transforms from the rocksalt (*B1*) to the CsCl-type (*B2*) structure at 120 kbar. CaTe also transforms to the *B2* structure near 350 kbar, however, with the possible existence of an intermediate unidentified phase at around 320 kbar. These results, together with known structural changes in other *IIa-VI* compounds, are used to outline empirical relations for the pressures necessary to stabilize the *B2* phase in these materials.

I. INTRODUCTION

A pressure-induced phase transition from the octahedrally coordinated rocksalt structure (*B1*) to the CsCl-type structure (*B2*) with eightfold coordination is a common phenomenon in alkali halides.¹⁻⁴ Recent high-pressure x-ray investigations of CaO,⁵ SrO,⁶ and Ba chalcogenides⁷⁻⁹ suggest that the heavy alkaline-earth chalcogenides (*AX*, *X*=O, S, Se, Te) form a second large group of partly ionic crystals undergoing *B1-B2* transitions within the pressure range accessible by diamond-anvil techniques. The high-pressure x-ray study of CaTe and SrTe described here is aimed at determining the pressure-volume (*PV*) relations and searching for the occurrence of structural changes in these two compounds, which among the heavy *AX* have the smallest cation-to-anion radius ratio, r_C/r_A .¹⁰

SrTe is found to undergo a *B1-B2* transition at 120 kbar with a relative volume change of 11.1%. The *B1* phase of CaTe is stable up to about 300 kbar and CaTe transforms to the *B2* structure near 350 kbar. X-ray diffraction patterns indicate the possible existence of an unidentified phase intermediate between *B1* and *B2* structures in CaTe.

The present work provides a broader experimental basis for a discussion of systematic trends of structural transitions in *AX*. In particular, there exists a simple empirical relation for the pressures necessary to stabilize the *B2* structure, which also applies to some of the divalent rare-earth monochalcogenides and *IV-VI* compounds.

II. EXPERIMENTAL PROCEDURE

High-pressure x-ray diffraction patterns of CaTe and SrTe were measured by using a gasketed diamond-anvil cell in combination with an angle-dispersive powder diffractometer. Pressures were determined from the red shift of the ruby *R*-line luminescence using a conversion factor of 0.365 A/kbar.¹¹ SrTe powder was prepared by grinding single crystalline material of light yellow color under argon gas. The single crystals of SrTe were grown from the melt. The dark polycrystalline starting material of CaTe was of nominal 99.5% purity. This material was used without any further chemical treatment. The

normal-pressure lattice constants of these samples (see Table I) are in close agreement with literature data. Samples were loaded into the gasket hole under inert gas without using a pressure medium.

III. EXPERIMENTAL RESULTS

High-pressure x-ray measurements of SrTe were performed up to 220 kbar. The onset of a crystallographic phase change is observed near 120 kbar (increasing pressure). Diffraction patterns of the high-pressure phase can be indexed as simple cubic (*B2*) with typical data listed in Table II. With increasing pressure, the *B1* phase is no longer observable above 140 kbar, while with decreasing pressure, the diffraction lines of the *B2* phase disappear completely below 100 kbar. Thus, we give the pressure P_T for the transition to the *B2* phase as 120 ± 10 kbar. Visual observation of SrTe reveals a reversible color change from deep yellow to nontransparent at the *B1-B2* transition.

The *PV* data for SrTe are shown in Fig. 1. The solid line corresponds to a least-squares fit of a Birch relation¹³

$$P(V) = 1.5B_{01}(X^7 - X^5)[1 - \eta(X^2 - 1)], \quad (1)$$

where $X = V/V_{01}^{-1/3}$ and $\eta = 3(1 - B'_{01}/4)$. V_{01} , B_{01} ,

TABLE I. Summary of experimental results for CaTe and SrTe. a_{01} , B_{01} , and B'_{01} are lattice constant, bulk modulus, and its pressure derivative, respectively, of the *B1* phases at normal conditions. V_{T1}/V_{01} , $\Delta V/V_{T1}$, and P_T are relative volume, relative volume change, and pressure, respectively, at the transition to the *B2* phase. V_{02}/V_{01} is the hypothetical zero-pressure volume of the *B2* phase.

	CaTe	SrTe
a_{01} (Å)	6.356 ± 0.001	6.659 ± 0.006
B_{01} (kbar)	420 ± 30	395 ± 30
B'_{01}	5	5
P_T (kbar)	350 ± 50	120 ± 10
$\Delta V/V_{T1}$ (%)	10.8 ± 1.0	11.1 ± 0.7
V_{T1}/V_{01}	0.703	0.828
V_{02}/V_{01}	0.865	0.876

TABLE II. Experimental and calculated x-ray diffraction data for SrTe and CaTe at 195 and 395 kbar, respectively. G denotes lines for which intensities and d values are uncertain due to a possible overlap with gasket lines.

$hk l$	d_{obs} (Å)	d_{calc} (Å)	I_{obs} (%)	I_{calc} (%)
SrTe at 198 kbar				
100		3.708	< 5	4
110	2.621	2.622	100	100
111		2.141		1
200	1.855	1.854	10	19
210		1.659		2
211	1.514	1.514	40	42
CaTe at 395 kbar				
100	3.388	3.387	18	27
110	2.395	2.397	100	100
111	G	1.955	G	9
200	G	1.693	G	18
210	1.514	1.515	10	13
211	1.383	1.383	25	39

and B'_{01} are volume, bulk modulus, and its pressure derivative, respectively, of the $B1$ phase (index 1) at normal density. With the parameters given in Table I, the standard deviation is 5 kbar.

X-ray diffraction studies of CaTe have been extended to 420 kbar. Starting near 320 kbar, new diffraction peaks occur which would fit a simple cubic indexing except for two additional reflections near the (110) peak. By increasing the pressure to 400 kbar, these two peaks disappear and the diffraction pattern develops into that of a simple cubic ($B2$) phase (see Table II). These observations indicate the possible existence of a phase intermediate between $B1$ and $B2$ structure in CaTe. On reducing pressure, the $B2$ phase remains predominant down to about 300 kbar. An undisturbed diffraction pattern of the $B1$ phase

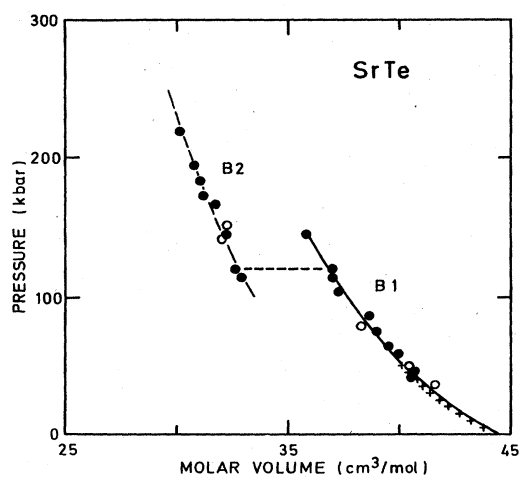


FIG. 1. Pressure-volume relation for SrTe. Closed and open circles correspond to increasing and decreasing pressure. Bridgman's data (Ref. 12) are indicated by crosses.

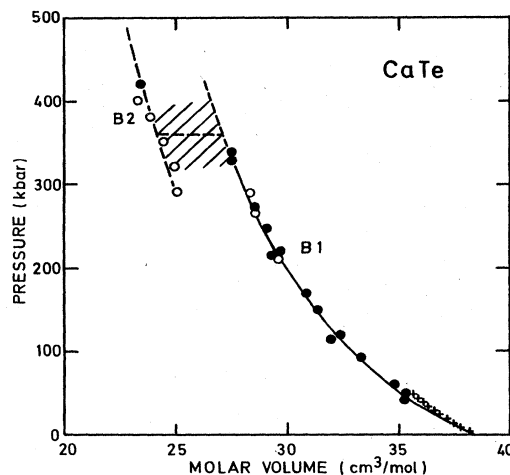


FIG. 2. Pressure-volume relation for CaTe. For explanation of symbols see Fig. 1. The shaded area indicates the region of the possible existence of an intermediate phase.

occurs again near 270 kbar. Due to the more complicated behavior of CaTe between 300 and 400 kbar, the transition pressure P_T is given as 350 kbar with a large uncertainty of ± 50 kbar. The PV relation of CaTe is shown in Fig. 2. The solid line ($B1$ phase) corresponds to a Birch relation (for parameters see Table I, where the standard deviation is 8 kbar).

The bulk moduli obtained for CaTe and SrTe and for other AX (Refs. 5–9, 14, and 15) fit into a systematic sequence. This is illustrated in Fig. 3 by plotting bulk modulus B_{01} versus molar volume V_{01} on a double-logarithmic scale. For comparison, data for alkali halides¹⁶ are also shown. Qualitatively, the physical origin of the straight-line relationships in Fig. 3 with slope $d \ln B_0 / d \ln V = -1.1$ can be traced back to elementary

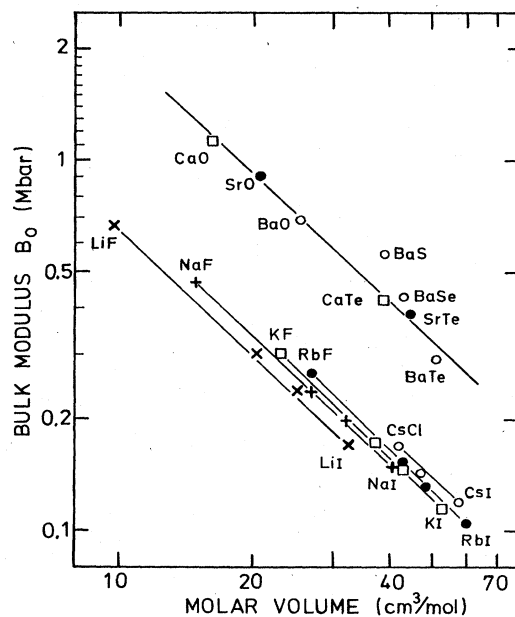


FIG. 3. Normal pressure bulk moduli of alkaline-earth chalcogenides and alkali halides as a function of molar volume.

concepts of ionic crystal physics.¹⁷ The bulk moduli of the *B2* compounds CsI, CsBr, and CsCl fit smoothly into the systematics for the *B1* alkali halides. Therefore, the bulk modulus scaling appears to be almost independent of crystal structure and we use the relation (index 2=*B2* phase)

$$B_{02} = B_{01} (V_{02}/V_{01})^{-1.1} \quad (2)$$

as a boundary condition in fitting a Birch relation to *PV* data for the high-pressure *B2* phases of CaTe and SrTe. If one assumes that $B'_{02} = B'_{01}$, the only remaining parameter is the hypothetical zero-pressure volume V_{02} of the *B2* phase. The corresponding Birch relations for the *B2* phases are shown by dotted curves in Figs. 1 and 2. In Table I we list V_{02}/V_{01} , the relative volume V_{T1}/V_{01} (*B1* phase) at the transition, and the relative volume change $\Delta V/V_{T1} = (V_{T1} - V_{T2})/V_{T1}$ as obtained from differences between fitted Birch relations.

IV. DISCUSSION

In Figs. 4 and 5, the experimental data related to the *B1*–*B2* transitions in CaTe and SrTe are compared to similar results reported for other *AX*.^{5–9,14} BaO is included here, because the PH_4I -type structure observed above 140 kbar (Ref. 14) (after a first transition to a tetragonal structure near 60 kbar) can be viewed as a distorted *B2* structure with eightfold coordination. The rel-

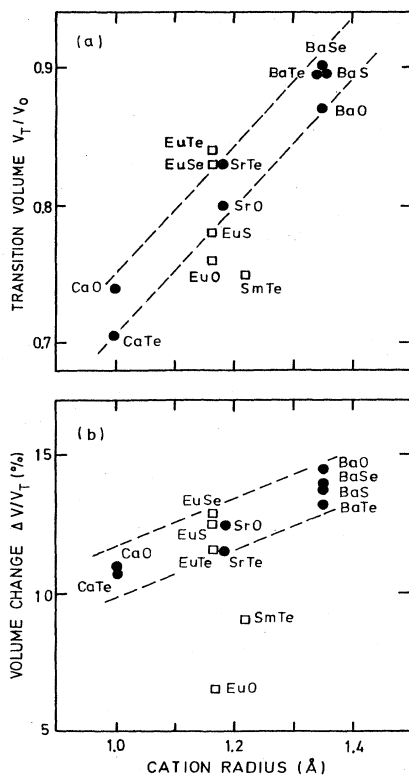


FIG. 4. (a) Relative volume V_{T1}/V_{01} (*B1* phase) and (b) relative volume change $\Delta V/V_{T1}$ of ionic monochalcogenides at the *B1*–*B2* transition (for BaO see text). Closed circles and open squares refer to alkaline-earth and rare-earth compounds.

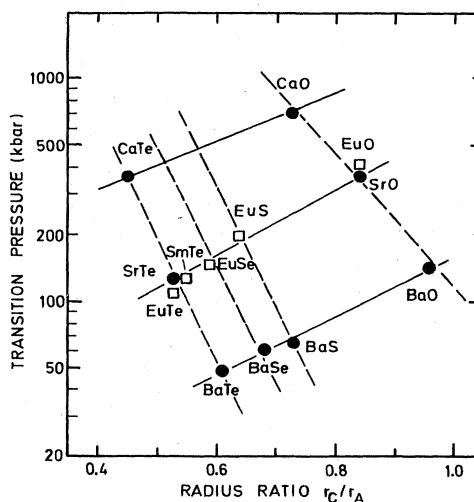


FIG. 5. Pressure at transition to eightfold-coordinated structure ($\cong B2$ except for BaO, see text) in ionic monochalcogenides plotted as a function of cation-anion radius ratio.

ative volume (*B1* phase) at the transition [Fig. 4(a)] decreases with smaller cation radius. The volume discontinuity [Fig. 4(b)] also tends to smaller values with decreasing cation radius. This overall correlation between V_{T1}/V_{01} and $\Delta V/V_{T1}$ may simply result from an increase in elastic energy terms with decreasing V_{T1}/V_{01} .

The pressures P_T necessary to stabilize the *B2* phase in *AX* exhibit a clear dependence on cation and anion radius. This is shown in Fig. 5 by plotting P_T versus radius ratio. Decreasing anion or cation radius requires an increasing transition pressure, however, at different slopes for either anion or cation variation. The pronounced tendency to higher transition pressures with decreasing cation radius is directly related to trends in V_{T1}/V_{01} [see Fig. 4(a)]. The decrease of P_T with increasing anion radius is correlated with decreasing zero-pressure binding energy and with increasing metallization (in the Mooser-Pearson sense¹⁸), if one moves down the chalcogenide row. A further correlation is that, for either cation or anion variation, P_T is lower for those compounds expected to have the smaller valence-band width in the *B1* phase.¹⁹ The valence-band width is in part a measure of the strength of the crystal field at the anion sites, as determined by the cation-anion distance, but also depends on anion-anion overlap, i.e., second-nearest-neighbor interactions.

In qualitative agreement with radius ratio rules,^{2,3} ionic *B1* compounds with a small radius ratio or a small electronegativity difference (e.g., NaBr, NaI) tend to first transform to structures with effective coordination numbers (CN) intermediate between CN=6 (*B1*) and CN=8 (*B2*).^{2–4} The possible existence of a phase intermediate between *B1* and *B2* structure in CaTe may be related to this tendency.

The data presented in Figs. 4 and 5 suggest that the systematics in transition volumes and pressures is also valid for the remaining SrX and CaX. From the empirical relations shown by solid and dashed lines in Fig. 5, one expects *B1*–*B2* transitions in SrS, SrSe, CaS, and CaSe at pressures of roughly 200, 150, 500, and 400 kbar, respec-

tively.

The pressure for the transition to the $B2$ phase approximately scales with

$$R_M^{-1} = (r_C^{-2} + r_A^{-2})^{1/2}. \quad (3)$$

Figure 6 shows a plot of R_M^{-1} versus ionic radius ratio. This scaling also places the Ia-VII array roughly into the right position to account for the $B1$ - $B2$ transition pressures of alkali halides²⁰ relative to those of the AX . We note that the relative arrangement of compounds in Fig. 6 bears a strong resemblance to St. John-Bloch-type structural maps, in which a charge transfer and a homopolar coordinate (defined through pseudopotential core radii) are used for a structural classification of binary compounds at normal conditions.²¹

A critical radius ratio $r_C/r_A = 0.5$ for direct $B1$ - $B2$ transitions^{2,3} is indicated by a shaded line in Fig. 6. Obviously, MgO is also a possible candidate for a $B1$ - $B2$ transition. For P_T in the heavy AX we find approximately

$$\ln P_T = 8(R_M^{-1} - 0.39), \quad (4)$$

where P_T is in kbar and R_M in Å. Extrapolation of this relation yields $P_T = 12$ Mbar for MgO. For comparison, pseudopotential calculations²² predict $P_T = 10$ Mbar, which seems to support the purely empirical rules lined out here.

The divalent radii of Eu and Sm differ by less than 0.03 Å from the Sr value.¹⁰ The systematics for $B1$ - $B2$ transition volumes and pressures proposed for the SrX applies to EuS, EuSe, and EuTe (see Figs. 4 and 5) which transform to the $B2$ phase near 200, 140, and 110 kbar, respectively.²³ EuO [$P_T = 400$ kbar (Ref. 23)] as well as SmTe [$P_T = 110$ kbar (Ref. 24)] are in the intermediate valence state (fractional 4f shell occupation) prior to the onset of the $B1$ - $B2$ transition. This explains the small relative volumes and volume changes of these two compounds at their $B1$ - $B2$ transitions [see Figs. 4(a) and 4(b)]. The coincidence of transition pressures for SrTe and SmTe does not imply that all intermediate valence SmX follow the empirical rules for the AX .

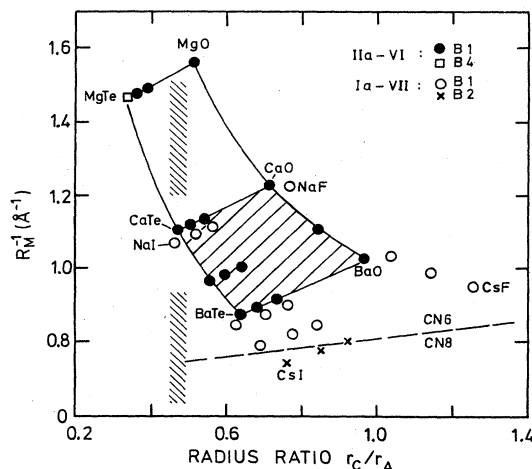


FIG. 6. Empirical coordinate R_M^{-1} [Eq. (3)] as a function of cation-anion radius ratio r_C/r_A for AX and alkali halides.

The divalent radius of lead is also close to that of Sr.¹⁰ The compounds PbTe, PbSe, and PbS transform from high-pressure orthorhombic phases (GeS-type) to the $B2$ phase at 130, 160, and 215 kbar, respectively.²⁵ These pressures fall on the "Sr line" in Fig. 5. SnTe with a divalent cation radius similar to Ca transforms to the $B2$ structure near 250 kbar,²⁶ which, on the logarithmic scale used in Fig. 5, is only a slightly lower pressure than CaTe.

In summary, the present results for CaTe and SrTe together with those from previously known structural transitions in IIa-VI compounds are used to formulate empirical relations for the pressures necessary to stabilize the $B2$ phase in these materials. The same empirical relations approximately hold for divalent rare-earth and group-IV chalcogenides, as far as they have been investigated by high-pressure x-ray diffraction in the appropriate pressure range.

ACKNOWLEDGMENT

We are grateful to K. Fischer (Jülich) for providing us with samples of SrTe.

¹See W. F. T. Pistorius, *Prog. Solid State Chem.* **11**, 1 (1976), for a review of work before 1975.

²H. H. Demarst, Jr., C. R. Cassell, and J. C. Jamieson, *J. Phys. Chem. Solids* **39**, 1211 (1978).

³T. Yagi, T. Suzuki, and S. Akimoto, *J. Phys. Chem. Solids* **44**, 135 (1983).

⁴Y. Sato-Sorensen, *J. Geophys. Res.* **88**, 3543 (1983).

⁵R. Jeanloz, T. Ahrens, H. K. Mao, and P. M. Bell, *Science* **206**, 829 (1979).

⁶Y. Sato and R. Jeanloz, *J. Geophys. Res.* **86**, 11 (1981); **86**, 773 (1981).

⁷S. Yamaoka, O. Shimomura, H. Nakazawa, and O. Fukunaga, *Solid State Commun.* **33**, 87 (1980).

⁸T. A. Grzybowski and A. L. Ruoff, *Phys. Rev. B* **27**, 6502 (1983).

⁹T. A. Grzybowski and A. L. Ruoff, *Phys. Rev. Lett.* **53**, 489 (1984).

¹⁰R. D. Shannon, *Acta Crystallogr., Sect. A* **32**, 751 (1976).

Throughout this work we refer to sixfold-coordinated ionic radii.

¹¹G. J. Piermarini, S. Block, J. D. Barnett, and R. A. Forman, *J. Appl. Phys.* **46**, 2774 (1975).

¹²P. W. Bridgman, *Collected Experimental Papers* (Harvard University Press, Cambridge, 1964).

¹³F. Birch, *J. Geophys. Res.* **83**, 1257 (1978).

¹⁴L. G. Liu and W. A. Bassett, *J. Geophys. Res.* **77**, 4934 (1972).

¹⁵L.-G. Liu and W. B. Bassett, *J. Geophys. Res.* **78**, 8470 (1973).

¹⁶See compilation of data by A. L. Ruoff and L. C. Chhabildas, in *High Pressure Science and Technology*, edited by K. D. Timmerhaus and M. S. Barber (Plenum, New York, 1979).

¹⁷M. O'Keeffe, in *Structure and Bonding in Crystals*, edited by M. O'Keeffe and A. Navrotsky (Academic, New York, 1981), Vol. 1, p. 299; A. Jayaraman, B. Batlogg, R. G. Maines, and H. Bach, *Phys. Rev. B* **26**, 3347 (1982).

¹⁸E. Mooser and W. B. Pearson, *Acta Crystallogr.* **12**, 1015

- (1959).
- ¹⁹S. T. Pantelides, *Phys. Rev. B* **11**, 5082 (1975).
- ²⁰*B* 1–*B* 2 transition pressures (in kbar) for alkali halides are (from Refs. 1–4) NaF 270, NaCl 290, KF 40, KCl 19.3, KBr 17.4, KI 19, RbF 30, RbCl 5.2, RbBr 4.0, RbI 3.5, CsF 20.
- ²¹J. St. John and A. N. Bloch, *Phys. Rev. Lett.* **33**, 1095 (1974); J. R. Chelikowsky and J. C. Phillips, *Phys. Rev. B* **17**, 2453 (1978); A. Zunger and M. L. Cohen, *ibid.* **20**, 4082 (1979).
- ²²K. J. Chang and M. L. Cohen, *Phys. Rev. B* **30**, 4774 (1984).
- ²³A. Jayaraman, A. K. Singh, A. Chatterjee, and S. U. Devi, *Phys. Rev. B* **9**, 2513 (1974); A. Jayaraman, *Phys. Rev. Lett.* **29**, 1674 (1972).
- ²⁴A. Chatterjee, A. K. Singh, and A. Jayaraman, *Phys. Rev. B* **6**, 2285 (1972).
- ²⁵T. Chattopadhyay, A. Werner, and H. G. von Schnering, in *High Pressure in Science and Technology*, edited by G. C. Homan, R. K. MacCrone, and E. Whalley (North Holland/Elsevier, New York, 1984), Vol. III, p. 93; Y. Fujii, K. Kitamura, A. Onodera, and A. Yamada, *Solid State Commun.* **49**, 135 (1984).
- ²⁶K. Murata, A. Onodera, Y. Fujii, Y. Yamada, T. Yagi, and S. Akimoto, in *Solid State Physics Under Pressure*, edited by S. Minomura (Reidel, Dordrecht, 1985).